Structure of the intermediate phase of PbTe at high pressure

G. Rousse,[1,*] S. Klotz,[1] A. M. Saitta,[1] J. Rodriguez-Carvajal,[2] M. I. McMahon,[3] B. Couzinet,[1] and M. Mezouar[4]
[1]*Physique des Milieux Denses, Institut de Minéralogie et de Physique des Milieux Condensés, CNRS UMR 7590–Universités Paris 6-Paris 7-IPGP, Campus Boucicaut, 140 Rue de Lourmel, 75015 Paris, France*
[2]*Laboratoire Léon Brillouin (CEA-CNRS), CEA/Saclay, 91191 Gif sur Yvette Cedex, France*
[3]*School of Physics and Centre for Science at Extreme Conditions, The University of Edinburgh, Kings Buildings, Edinburgh EH9 3JZ, United Kingdom*
[4]*European Synchrotron Radiation Facility, Boîte Postale 220, 38042 Grenoble, France*
(Received 19 November 2004; published 29 June 2005)

The evolution of PbTe with pressure has been reexamined using synchrotron x-ray diffraction. The phase transition at 6 GPa is not to the GeS (B16) or TlI (B33) type structures, as previously reported, but to an orthorhombic *Pnma* structure, with cell parameters $a=8.157(1)$, $b=4.492(1)$, and $c=6.294(1)$Å at 6.7 GPa. This structure corresponds to a distortion of the low-pressure NaCl structure with a coordination intermediate between the sixfold B1 (NaCl) and the eightfold B2 (CsCl) structure. We discuss the stability of this new structure with respect to other proposed phases using numerical methods. These results may modify the admitted paths of phase transitions between the B1 and B2 structures.

DOI: 10.1103/PhysRevB.71.224116 PACS number(s): 61.10.Nz, 61.50.Ks, 81.05.Hd

I. INTRODUCTION

The lead chalcogenides PbX (X=Te, Se, S) are narrow-gap semiconductors (group IV–VI), which crystallise at ambient conditions in the cubic NaCl (B1) structure. They are extensively used in Peltier elements, infrared detectors, diode lasers,[1] and in thermophotovoltaic energy converters.[2] High-pressure experimental data on their structure and lattice dynamics provide crucial tests for modeling semiconductors by computational techniques.[3–6] The IV-IV and III-V semiconductors have been extensively studied under pressure and are well understood.[7] The situation is very different for the sixfold-coordinated cubic systems of prototype PbX. Structural transitions in PbTe, PbSe, and PbS were first reported by Bridgman in 1940.[8] Later diffraction work confirmed that PbTe, PbSe, and PbS transform at 6, 4.5, and 2.2 GPa, respectively, to an intermediate phase, and beyond (between 13 and 22 GPa) to the eightfold-coordinated CsCl (B2) structure.[9,10] The intermediate phase has been referred to as being of the "GeS" type (B16, space group *Pbnm*) rather than of the "TlI" type, as suggested for PbS and PbSe (B33, space group *Cmcm*),[11] but there is evidence that this is incorrect.[9,10,12–14] This is in contrast to computational results,[15] which affirm that all three systems—PbTe, PbS, and PbSe—indeed adopt the TlI structure. It hence appears that 65 years after Bridgman's discovery, the question of the structure of these phases is still unsettled. Our interest in the structural aspects of the intermediate phases arose out of lattice-dynamical studies of the NaCl structure of PbTe under pressure, where a pronounced softening of the transverse acoustic phonon branches in [100] and [110] directions was observed.[16] This may well be related to structural features of the intermediate phase.[4]

In this paper, we report x-ray powder diffraction obtained at synchrotron sources which allowed us to solve the structure of the intermediate phase of PbTe. *Ab initio* calculations have been carried out to investigate the relative stability of the proposed structure with respect to the NaCl and the GeS type structures.

II. EXPERIMENTAL AND THEORETICAL METHODS

High-purity PbTe powder samples (99.999%) provided by Alfa were used in the experiments. One data set was collected on station ID30 of the European Synchrotron Radiation Facility (ESRF) at 300 K using an image plate detector and with a wavelength of $\lambda=0.3738$ Å. The diamond anvil pressure cell was loaded with a 4:1 methanol-ethanol mixture as a pressure transmitting medium. Stainless steel gaskets provided a sample hole of 120 μm. A second set of data has been collected at the Synchrotron Radiation Source (SRS) at Daresbury Laboratory using an image plate detector and an incident wavelength of $\lambda=0.4654$ Å.[17] In both cases, the pressure was determined to a precision of $+/-0.2$ GPa using the ruby fluorescence technique. The program FULLPROF[18] was used for crystal structure refinements using the Rietveld method.[19]

Ab initio calculations have also been performed in order to obtain an insight into the phase transitions at the atomic level and on the local structure and energetics of the intermediate phases. Our calculations have been carried out within the density-functional theory and the local-density approximations. We adopted a standard plane-wave/pseudopotential approach as implemented in the PWSCF code.[20] Both pseudopotentials were built according to the von Barth–Car scheme; nonlinear core corrections were included in the Pb description. A 30 Ry cutoff and $4\times4\times4$ k-point grids were used in the rocksalt phase; finer grids and Methfessel-Paxton broadening were used in the study of the intermediate- and high-pressure structures.

III. RESULTS AND DISCUSSION

The quality of our sample has been verified by the analysis of the data recorded once the pressure cell was sealed at 0.4 GPa. The refinement of the NaCl structure [$Fm\bar{3}m$, Pb at (0.5 0.5 0.5), Te at (0 0 0)] leads to a lattice parameter of

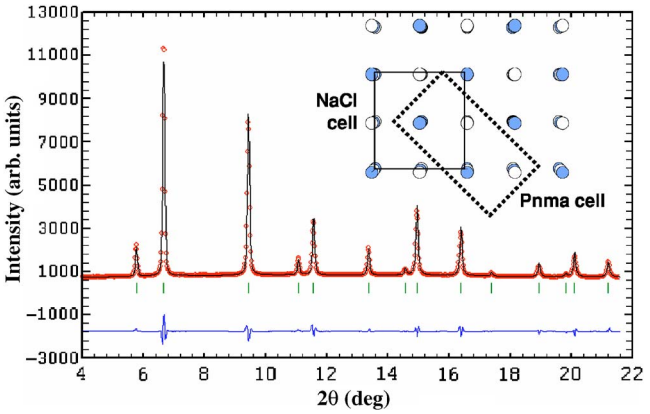

FIG. 1. Rietveld refinement of the NaCl phase of PbTe, recorded at 0.4 GPa, at ESRF (λ=0.3738 Å). Dots are data points, vertical bars are the Bragg positions. The continuous line is the calculated pattern. Inset: Structure of the NaCl phase of PbTe. Open circles are Pb atoms, filled circles are Te atoms. The NaCl cell is indicated. The dotted lines indicate the intermediate *Pnma* cell of PbTe at high pressure (see Sec. III B) .

6.4245(4) Å. The temperature factors were refined to 1.29(5) and 0.83(7) Å^2 for Pb and Te, respectively. No impurity is detected, as shown in Fig. 1.

On increasing pressure, a first-order phase transition to the "intermediate phase" was observed between 6 and 7 GPa. Figure 2 shows a pattern recorded at 6.7 GPa at the ESRF together with the calculated patterns from the TlI and GeS type structures. Note that although the observed pattern from the intermediate pressure phase of PbTe is similar to the one observed in Ref. 12, the reflections, in particular the strong reflection at Q=2.3 Å^{-1}, cannot be indexed on the previously suggested TlI or GeS structures. This had already been pointed out by both MacLean[21] and Chattopadhyay.[12] Another report by Onodera *et al.*[14] has discussed the possibility of indexing the intermediate phase using the SnTe-II structure, that is, an orthorhombic cell with lattice parameters a=8.166, b=8.802, and c=6.190 Å. However, no space group or structural model was proposed, and the structure of the intermediate phase thus remained unsolved.

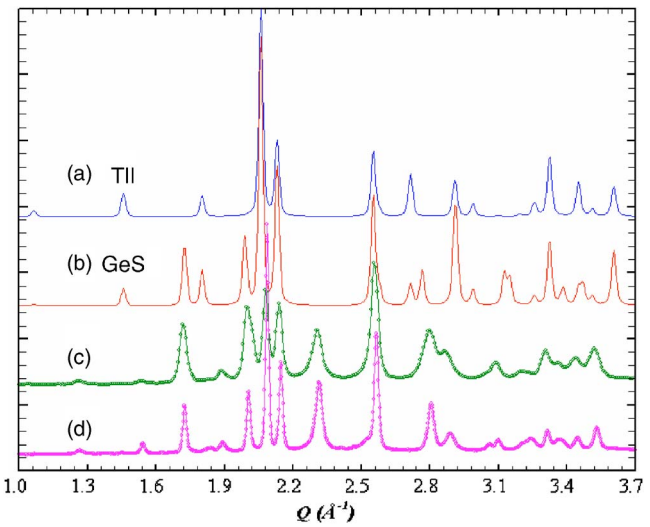

FIG. 2. (a) and (b) Calculated patterns for PbTe with the TlI and the GeS type structure. (c) Observed pattern of PbTe at 6.7 GPa at ESRF. (d) Pattern recorded at SRS, after annealing at 200 °C for 14 h, for which the pressure had dropped from 8.8 to 6.5 GPa.

A. Structure of the intermediate phase of PbTe at high pressure

The PbTe pattern measured at 6.7 GPa at the ESRF was indexed using Dicvol 91.[22,23] Several different unit cells were found, and in each case we refined the profile without a structural model (profile matching or Le Bail fit). For each trial cell, the atomic volume was compared to that deduced from the measured density, at the same pressure, obtained using volumetric measurements.[8] From the comparison it was concluded that only two unit cells need to be considered further, an orthorhombic cell with a=8.157(1), b=4.492(1), and c=6.294(1) Å, and a monoclinic distortion of this cell, both with Z=4. Profile matching refinements showed, however, that the goodness of fit did not significantly improve by relaxing the symmetry to monoclinic. The orthorhombic cell thus appeared to be the most likely solution. Note that this cell is completely different from that previously reported for the GeS or TlI type structures. Interestingly, this cell is, however, half the cell proposed by Onodera *et al.*[14]

The distribution of the atoms within the unit cell was then determined by using the simulated annealing technique (*SAnn*) (Ref. 24) implemented in FULLPROF. The relative positions of the eight atoms within the unit cell were considered without symmetry constraints. An optimal distribution of atoms was chosen by eliminating some unrealistic atomic distributions that were also provided by *SAnn* in different runs. The space group was obtained by considering only the most symmetric structure consistent with the atom distribution obtained from *SAnn*. Two final possibilities were found, both with space group *Pnma* and lattice parameters a=8.177 Å, b=4.495 Å, c=6.230 Å, and Pb and Te atoms on the 4c site, Pb (0.82, 0.25, −0.19) Te (0.56, 0.75, 0.87) and Pb (0.56, 0.25, −0.19) Te (0.82, 0.75, 0.87).

These two possibilities differ only by the x coordinate of Pb and Te, which are inverted. The refinement of the ESRF data using the first or the second choice gave very similar results, with a slightly better refinement for the second structural model. In order to distinguish both structures, simulations based on electronic structure calculations were carried out. The second structure was indeed found to be more stable than the first one: the first transforms into the second if the atom coordinates are relaxed.

The refinement with the second model is shown in the inset of Fig. 3. Preferred orientation had to be introduced along [100] to improve the refinement. A procedure based in the March-Dollase-Wright (see Ref. 25) multiaxial model for preferred orientation adapted for image plate high-pressure anvil cells in synchrotron beamlines was used (Nor=3 in FULLPROF). The sample suffers also from microstructural effects, as clearly seen in the anisotropic peak broadening and small shifts of several reflections. A refinement of the peak broadening using a quartic *hkl* dependence of the Gaussian and Lorentzian full width at half maximum (FWHM) (see

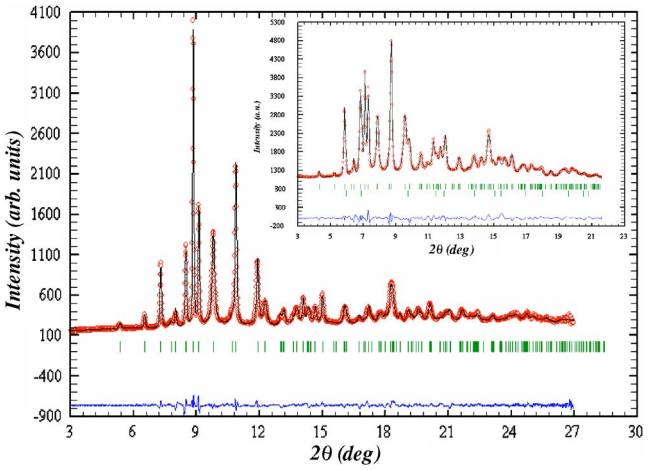

FIG. 3. Rietveld refinement of the intermediate phase of PbTe at high pressure at 6.5 GPa from SRS data after annealing 14 h at 200 °C (λ=0.4654 Å). Inset: Rietveld refinement of the intermediate phase of PbTe at high pressure from ESRF data, at 6.7 GPa (λ=0.3738 Å). Dots are data points, vertical bars are the Bragg positions. The continuous line is the calculated pattern. Note that there is a small amount of untransformed NaCl phase present in the ESRF data (lower tick marks).

Refs. 26 and 27) improves the fit but does not fully account for all the microstructural effects. As we will see below, the peak broadening contains a part that is extrinsic to the sample, coming presumably from pressure gradients across grain boundaries. For this reason we have preferred to handle the microstructural effects in a phenomenological way by relaxing the peak broadening and shifts of the most affected reflections with respect to the average resolution parameters. This procedure provided a better estimation of some integrated intensities improving, without changing essentially, the structural parameters. The sample also proved to contain a remaining fraction of untransformed ambient pressure phase with lattice parameter $a=6.221$ Å. The final structural parameters are given in Table I. Occupation factors of Pb and Te were refined, but imposed that the sum equals 1 (no vacancies). The refinements indicate a non-negligible amount of atomic disorder: 10% of Pb on the Te site, and vice versa.

Apart from not being single phase, the ESRF data set proved to be strongly textured. For this reason, a second series of experiments was carried out at the SRS synchrotron at Daresbury, UK (λ=0.4654 Å). PbTe was compressed in a Merrill-Bassett cell using a 4:1 ethanol methanol mixture and a tungsten gasket. At 8.8 GPa, the sample was found to be the pure intermediate phase. Two other data sets were recorded after annealing the sample at 200 °C for 4 h and 14 h, without subsequent changes, except that the pressure dropped to 6.8 GPa and 6.5 GPa, respectively. The main difference between SRS and ESRF data is the intensity of the central peak in the triplet at $q=2.1$ Å^{-1}, as can be seen in Fig. 2. This is directly related to the preferred orientation along [100].

The quality of the refinement of the SRS data using our structural model is excellent and confirms the proposed structure (Fig. 3). The refinements of the other two patterns recorded after annealing are similar, and some preferred orientation along [100] has to be taken into account as well, although this phenomenon is less pronounced than in ESRF data. Here again, microstructural effects were taken into account using the same procedure as for the ESRF data. Here, due to the more effective resolution, we had to relax the FWHM and shifts of more reflections than in the case of the ESRF data. The reflections of the SRS pattern are differently affected by the microstructural effects, as should be the case for an extrinsic origin of the peak broadening. In this sample, the chemical Pb/Te disorder is much lower (4%). We report the structural refinement for the two data sets in Table I.

TABLE I. Structural parameters of the intermediate phase of PbTe at high pressure, from synchrotron (ESRF or SRS) x-ray powder diffraction. ESRF: recorded at 6.7 GPa; SRS: recorded after annealing at 200 °C for 14 h; the pressure had then dropped from 8.8 to 6.5 GPa. B are the isotropic temperature factors (Å^2). "Pb/Te antisite" corresponds to the percentage of atoms of the wrong species occupying the crystallographic site of the other.

Sample pressure	PbTe ESRF 6.7 GPa	PbTe SRS 6.5 GPa
Space group	*Pnma*	*Pnma*
Lattice parameter a (Å)	8.157(1)	8.152(1)
Lattice parameter b (Å)	4.492(1)	4.486(1)
Lattice parameter c (Å)	6.294(1)	6.284(1)
Cell volume (Å^3)	230.6	229.8
x(Pb)	0.564(1)	0.565(1)
y(Pb)	0.25	0.25
z(Pb)	−0.189(1)	−0.192(1)
x(Te)	0.821(1)	0.828(1)
y(Te)	0.75	0.75
z(Te)	0.868(1)	0.863(1)
B(Pb)	1.21(5)	2.24(4)
B(Te)	1.1(1)	1.5(1)
Pb/Te antisite	10%	4%

B. Relation with the low-pressure NaCl structure

The structure of the intermediate phase of PbTe at high pressure is related to the low-pressure NaCl phase by the following operations:

$$\mathbf{a}_{\mathrm{PbTe}} = \mathbf{a}_C - \mathbf{b}_C,$$

$$\mathbf{b}_{\mathrm{PbTe}} = (\mathbf{a}_C + \mathbf{b}_C)/2,$$

$$\mathbf{c}_{\mathrm{PbTe}} = \mathbf{c}_C, \tag{3.1}$$

where the subscript PbTe refers to the orthorhombic *Pnma* cell, and C to the low-pressure cubic NaCl cell, and a change in origin by (1/4, 1/2, 3/4) in the NaCl cell has to be taken into account. In the intermediate structure at high pressure, atoms are slightly displaced in the (a,c) plane of the *Pnma* cell to be distributed on the 4c positions of *Pnma*. In Fig. 4, where three views of the proposed structure are displayed,

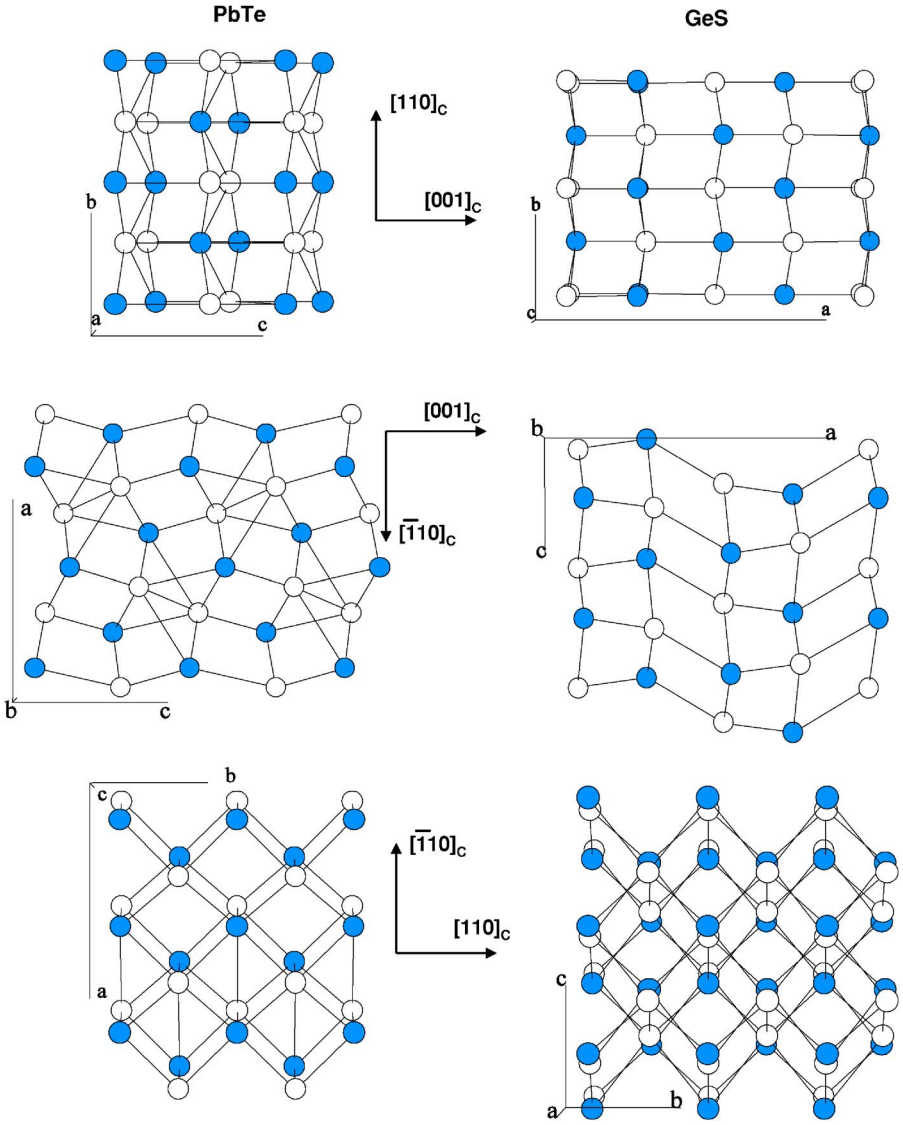

FIG. 4. Structure of the intermediate phase of PbTe at high pressure (left) and of the GeS type structure (right). Open circles are Pb atoms, filled circles are Te atoms. Three views are displayed: perpendicular to the $[\bar{1}10]_c$ (top), $[110]_c$ (middle), and $[001]_c$ (bottom) NaCl cubic axes. Note that the major atomic displacements are along $[001]_c$ for PbTe, whereas they are along $[\bar{1}10]_c$ for the GeS type. One can also notice the difference in coordination in the view perpendicular to the $[110]_c$ axis: it is 7 for PbTe and 6 for the GeS type structure.

one can note that, the linear arrangement of Pb and Te atoms in the NaCl phase becomes "modulated" in the high pressure *Pnma* phase. Pb and Te atoms are still successively disposed, but these slight displacements in the (a,c) plane create a modulation. The displacements of atoms are of about 0.4–0.5 Å in the a and c directions, as compared to the cubic positions. The NaCl to *Pnma* transition can hence be regarded as displacive, although being of first-order.

The atomic displacements are nevertheless large enough to modify considerably the atomic coordinations with respect to the NaCl structure. Pb (Te) atoms are surrounded by 7 Te (Pb) atoms, as well as two Pb (Te) atoms at slightly larger distances. At 6.5 GPa, the seven neighbors of a different kind are located at distances ranging from 2.93 to 3.81 Å. Note that the coordination of 7 is intermediate between the high-symmetry NaCl and high-pressure CsCl structure, which are, respectively, sixfold- and eightfold-coordinated. There are 12 Te-Te and Pb-Pb distances, as in the NaCl and CsCl structures. These distances range from 3.46 to 4.89 Å for Pb atoms, and from 3.97 to 5.80 Å for Te atoms.

C. Comparison with the previously suggested structures GeS and TlI

As shown below, the previously proposed GeS type structure for the intermediate phase of PbTe, in spite of having the same space-group symmetry, is clearly different from the structure determined in this work. The volume of both cells is the same: the a lattice parameter is about twice that of the c lattice parameter of GeS, whereas our c lattice parameter is half that of a in GeS,

$$\mathbf{a}_{\mathrm{GeS}} = 2\mathbf{c}_{\mathrm{PbTe}}, \quad \mathbf{b}_{\mathrm{GeS}} = \mathbf{b}_{\mathrm{PbTe}}, \quad \mathbf{c}_{\mathrm{GeS}} = -\frac{1}{2}\mathbf{a}_{\mathrm{PbTe}}. \quad (3.2)$$

Figure 4 shows three views of the GeS structure together with the intermediate structure of PbTe at high pressure. The two structures differ in the way the atoms are displaced from the ideal B1 structure. For GeS, the cell is doubled along $[001]_c$ (the subscript c refers to the cubic NaCl cell), and the major atomic displacements are in the $[\bar{1}10]_c$ direction. In the intermediate structure of PbTe, however, the doubling of the

cell is along the $[\bar{1}10]_c$ direction and the major atomic displacements are along $[001]_c$, i.e., both are distortions of the NaCl structure, but in different directions. A major difference exists in the coordination: in the GeS structure, each atom is surrounded by six different atoms (as in the NaCl B1 structure), whereas the coordination is 7 in the intermediate structure of PbTe.

Note that the TlI structure (space group *Cmcm*), which was previously reported as the structure of the intermediate phase for PbTe at high pressure by numerical calculations,[15] is related to the GeS-type structure (space group *Pnma*) by the following relations:

$$\mathbf{a}_{\mathrm{TlI}} = \mathbf{c}_{\mathrm{GeS}}, \quad \mathbf{b}_{\mathrm{TlI}} = \mathbf{a}_{\mathrm{GeS}}, \quad \mathbf{c}_{\mathrm{TlI}} = \mathbf{b}_{\mathrm{GeS}}. \tag{3.3}$$

TlI can then be described in the *Pnma* space group of GeS, and by setting the z coordinate of Pb (Te) to 0 (1/2). Each atom is surrounded by five close neighbors of a different species below 3.5 Å, and by two others at a larger distance. The coordination of TlI can then be regarded as 5 or 7.

D. Stability of the intermediate phase at high pressure with respect to B1, B2, B16, and B33

The *ab initio* calculations predict, for the rocksalt phase, a lattice parameter of a=6.34 Å and a bulk modulus of 48.5 GPa, in typical LDA agreement with the experimental data of 6.46 Å and 39.8 GPa and previous calculations.[3,5,15] The theoretical study of the intermediate phases at high pressure shows that both the TlI and *Pnma* structures are more stable than the GeS phase; it is, however, difficult to predict which one is the most stable, since their enthalpy difference is within the estimated error of the calculations. Our calculations correctly predict a phase transition from the rocksalt structure to the *Pnma* phase at around 6.9 GPa, slightly higher than the experimental transition pressure. A second transition to the CsCl structure is predicted at 17.3 GPa, very close to the experimental value of 16 GPa.[9]

IV. CONCLUSIONS

We have shown, using Rietveld refinement of synchrotron x-ray powder diffraction, that the intermediate phase of PbTe at high pressure is not of GeS or TlI type, as previously reported. PbTe has an orthorhombic *Pnma* structure between 6 and 16 GPa, which is a modulated deformation of the low-pressure NaCl structure. This is the first time, to our knowledge, that such a structure has been reported as intermediate between the B1 and B2 phases. This structure has not previously been considered in discussions of the transition path between the two phases.[28,29] Our study could help in understanding the observed transitions in binary compounds such as monochalcogenides, monopnictides, and monohalides.

The fact that the intermediate structures of PbX compound are modulated distortions of the NaCl structure may have an implication in the behavior of the phonon dispersion of the NaCl phase under pressure, as was already pointed out by Cochran *et al.*[4] In measurements of the lattice dynamics of PbTe, we have indeed found a pressure-induced softening of the transverse acoustic phonon branches in [100] and [110] directions,[16] which may be related to structural aspects of the high-pressure phase identified in this paper. Since the intermediate structure of PbTe is shown to be different from the one adopted by PbSe (which appears to be indeed of GeS type[21]), the details of the pressure-induced phonon softening may be significantly different as well.

ACKNOWLEDGMENTS

The authors are grateful to P. Bouvier for help during the experiments. Nonallocated beamtime for the present study has been kindly provided by the ESRF. This work at SRS was supported by grants from EPSRC, funding from CCLRC, and facilities provided by Daresbury Laboratory. M.I.M. acknowledges support from the Royal Society. The theoretical calculations have been performed at the IDRIS French National Computational Facility under the project 11387-CP9 and renewals.

*Corresponding author. Email address: gr@pmc.jussieu.fr

[1] H. Preier, Appl. Phys. **20**, 189 (1979).
[2] T. K. Chaudhuri, Int. J. Energy Res. **16**, 481 (1992).
[3] S. H. Wei and A. Zunger, Phys. Rev. B **55**, 13 605 (1997).
[4] W. Cochran, R. A. Cowley, G. Dolling, and M. M. Elcombe, Proc. R. Soc. London, Ser. A **293**, 433 (1966).
[5] M. Lach-hab, D. A. Papaconstantopoulos, and M. J. Mehl, J. Phys. Chem. Solids **63**, 833 (2002).
[6] M. Lach-hab, M. Keegan, D. A. Papaconstantopoulos, and M. J. Mehl, J. Phys. Chem. Solids **61**, 1639 (2000).
[7] M. I. McMahon and R. J. Nelmes, Phys. Status Solidi B **198**, 389 (1996).
[8] P. W. Bridgman, Proc. Am. Acad. Arts Sci. **74**, 21 (1940).
[9] Y. Fujii, K. Kitamura, A. Onodera, and Y. Yamada, Solid State Commun. **49**, 135 (1984).
[10] T. Chattopadhyay, A. Werner, and H. G. von Schnering, Rev. Phys. Appl. **19**, 807 (1984).
[11] P. D. Hatton, J. R. Maclean, R. O. Piltz, J. Crain, and R. J. Cernik, *Experimental Report*, Daresbury Lab. (1994), p. 422.
[12] T. Chattopadhyay, H. G. von Schnering, W. A. Grosshans, and W. B. Holzapfel, Physica B & C **139-140**, 356 (1986).
[13] T. Chattopadhyay, J. Pannetier, and H. G. von Schnering, J. Phys. Chem. Solids **47**, 879 (1986).
[14] A. Onodera, Y. Fujii, and S. Sugai, Physica B & C **139-140**, 240 (1986).
[15] R. Ahuja, Phys. Status Solidi B **235**, 341 (2003).
[16] S. Klotz, Z. Kristallogr. **216**, 420 (2001).
[17] R. J. Nelmes and M. I. McMahon, J. Synchrotron Radiat. **1**, 69 (1994).
[18] J. Rodríguez-Carvajal, Physica B **192**, 55 (1993). For a more recent version, see J. Rodríguez-Carvajal, Recent Developments of the Program FULLPROF, in Commission on Powder Diffraction

(IUCr), Newsletter 26, 12-19, 2001, available at http://journals.iucr.org/iucr-top/comm/cpd/Newsletters/. The complete program and documentation can be obtained from the anonymous ftp-site: ftp://ftp.cea.fr/pub/llb/divers/fullprof.2k.

[19] H. M. Rietveld, J. Appl. Crystallogr. **2**, 65 (1969).

[20] http://www.pwscf.org

[21] J. R. Maclean, P. D. Hatton, R. O. Piltz, and R. J. Cernik, Nucl. Instrum. Methods Phys. Res. B **97**, 354 (1995).

[22] D. Louer and M. Louer, J. Appl. Crystallogr. **5**, 271 (1972).

[23] A. Boultif and D. Louer, J. Appl. Crystallogr. **24**, 987 (1991).

[24] S. Kirpatrick, C. D. Gelatt, and M. P. Vecchi, Science **220**, 671 (1983).

[25] N. Wright, R. J. Nelmes, S. Belmonte, and M. I. McMahon, J. Synchrotron Radiat. **3**, 112 (1996).

[26] J. Rodríguez-Carvajal, M. T. Fernandez-Diaz, and J. L. Martinez, J. Phys.: Condens. Matter **3**, 3215 (1991).

[27] P. Stephens, J. Appl. Crystallogr. **32**, 281 (1999).

[28] P. Toledano, K. Knorr, L. Ehm, and W. Depmeier, Phys. Rev. B **67**, 144106 (2003).

[29] D. Zahn and S. Leoni, Z. Kristallogr. **219**, 345 (2004).